

Geometrical picture of dynamical facilitation

Stephen Whitelam¹ and Juan P. Garrahan^{1,2}

¹*Theoretical Physics, University of Oxford, 1 Keble Road, Oxford, OX1 3NP, UK*

²*School of Physics and Astronomy, University of Nottingham, Nottingham, NG7 2RD, UK*

November 15, 2018

Abstract

Kinetically constrained models (KCMs) are models of glass formers based on the concept of dynamic facilitation. This concept accounts for many of the characteristics of the glass transition. KCMs usually display a combination of simple thermodynamics and complex glassy dynamics, the latter being a consequence of kinetic constraints. Here we show that KCMs can be regarded as systems whose configuration space is endowed with a simple energy surface but a complicated geometry. This geometry is determined solely by the kinetic constraints, and determines the dynamics of the system. It does not affect the overall distribution of states. Low temperature dynamical slow-down is then a consequence of the competition between the paths allowed by the geometry of configuration space, and those leading to energy relaxation. This competition gives rise to dynamical bottlenecks unrelated to static properties. This view of the dynamics is distinct from that based on an underlying static rugged energy landscape. We illustrate our ideas with simple examples.

1 Introduction

The view of the glass transition (see [1, 2, 3] for general reviews) as a dynamical phenomenon emerges naturally from the real-space picture of supercooled liquids developed in [4, 5, 6, 7, 8]. This work demonstrates that many of the properties of supercooled liquids can be simply explained by the existence and statistical properties of spatially correlated dynamics, or dynamical heterogeneity [9, 10, 11]. Dynamical heterogeneity has been observed both in deeply supercooled liquids [12], in the mildly supercooled regime in simulations [13], and in experiments on colloidal suspensions [14].

Heterogeneous dynamics, in combination with structural homogeneity, as observed in glass formers, appears in systems possessing both localized excitations and facilitated dynamics [15, 16, 17]. The concept of dynamic facilitation stipulates that the dynamics of a local region is suppressed if it is bordered by immobile regions, and thus reflects the idea that particles in a jammed liquid cannot rearrange unless adjacent to mobile particles. Dynamic facilitation is realized in KCMs, which are simple models of non interacting particles or excitations in a lattice whose dynamics is subject to kinetic constraints (see [18] for a review). Examples of KCMs are spin facilitated models, like the Fredrickson-Andersen (FA) model [17] or the East model [19], and constrained lattice gases, such as the Kob-Andersen model [20].

In this paper we study the effect that dynamic facilitation has on the geometry of configuration space, and how in turn this affects the dynamics [21]. We show, by generalizing KCMs to continuous degrees of freedom, that kinetic constraints impose a metric structure on configuration space which does not affect the static distribution of states, and therefore the thermodynamics, but which has a dramatic effect on the paths between states at low energies. We show that dynamical slow-down at low temperatures occurs because the

system is forced to evolve along configuration space paths of least metric distance, or geodesics, which are distinct from the paths that relax the energy. This competition between available trajectories and energy relaxation gives rise to dynamical barriers, or bottlenecks, which are unrelated to the statics of the system. This view of the dynamics is distinct from that based on the idea that a static rugged energy landscape is responsible for the properties of glass formers (see e.g. [3]).

This paper is organised as follows. In section 2 we discuss the geometric interpretation of dynamic facilitation. In sections 3 and 4 we illustrate our ideas with simple examples. In section 5 we state our conclusions.

2 Geometrical interpretation of constrained dynamics

The real-space picture of supercooled liquids of Refs. [4, 5, 6, 8] is based on two observations. First, at low temperature very few particles in the liquid are mobile, and these mobility excitations are localized in space. Second, regions of the liquid cannot become mobile unless their neighbouring regions are mobile. These observations are implemented as follows. A supercooled fluid in d spatial dimensions is coarse-grained into cells of linear size of the order of the static correlation length as given by the pair correlation function. Cells are classified by a scalar mobility field, x , identified by coarse-graining the system on a microscopic time scale. Mobile regions carry a free energy cost, and when mobility is low interactions between cells are not important. Adopting a thermal language, we expect static equilibrium to be determined by the non-interacting Hamiltonian,

$$H[x] = \sum_{\mu=1}^N f_{\mu}(x^{\mu}), \quad (1)$$

where $\mu = 1, \dots, N$ labels the lattice site, x^{μ} is the mobility field at site μ , and f_{μ} is an analytic function of x^{μ} chosen so that the ground state of the model is such that $|x^{\mu}|$ is small. At low mobility, the distinction between single and multiple occupancy is irrelevant, as is the distinction between discrete or continuous degrees of freedom. In what follows we assume x^{μ} to be real. The dynamics of the mobility field is given by a master equation,

$$\partial_t P(x, t) = \sum_{\mu} \mathcal{C}_{\mu}(x) \hat{\mathcal{L}}_{\mu} P(x, t), \quad (2)$$

where $P(x, t)$ is the probability that the system has configuration $x \equiv \{x^{\mu} \mid \mu = 1, 2, \dots, N\}$ at time t . The local operators $\hat{\mathcal{L}}_{\mu}$ are the same as those for unconstrained local dynamics. Their action on P can be written

$$\hat{\mathcal{L}}_{\mu} P(x) = \sum_{x'^{\mu}} w(x'^{\mu} \rightarrow x^{\mu}) P(x'^{\mu}, \{x^{\nu \neq \mu}\}) - \sum_{x'^{\mu}} w(x^{\mu} \rightarrow x'^{\mu}) P(x^{\mu}, \{x^{\nu \neq \mu}\}), \quad (3)$$

where $w(x^{\mu} \rightarrow x'^{\mu})$ is the probability of going from configuration $(x^{\mu}, \{x^{\nu \neq \mu}\})$ to configuration $(x'^{\mu}, \{x^{\nu \neq \mu}\})$ in unit time. We ensure a unique equilibrium configuration exists by requiring (2) to obey detailed balance with respect to (1), i.e.

$$\frac{w(x \rightarrow x')}{w(x' \rightarrow x)} = e^{-\beta(H[x'] - H[x])}. \quad (4)$$

The kinetic constraint, $\mathcal{C}_{\mu}(x)$, is designed to suppress the dynamics of cell μ when surrounded by immobile regions. It must also be such that Eq. (2) satisfies detailed balance, which is achieved if $\mathcal{C}_{\mu}(x)$ does not depend on x^{μ} itself. To reflect the local nature of dynamic facilitation we allow \mathcal{C}_{μ} to depend only on the $\{x^{\nu}\}$ of nearest neighbours of μ , and require that \mathcal{C}_{μ} is small when local mobility is scarce. Equations (1)-(4) define a generic KCM.

We now show that Eq. (2) has a simple geometrical interpretation. Using standard methods [22] we pass from the master equation (2) to the Fokker-Planck equation

$$\partial_t P(x, t) = \sum_{\mu} \mathcal{L}_{\mu}^{(\text{FP})} P(x, t), \quad (5)$$

where

$$\mathcal{L}_{\mu}^{(\text{FP})} = \frac{\partial}{\partial x^{\mu}} \left\{ \mathcal{C}_{\mu}(x) f'_{\mu}(x^{\mu}) + T \frac{\partial}{\partial x^{\mu}} \mathcal{C}_{\mu}(x) \right\}. \quad (6)$$

The prime on f_{μ} denotes differentiation with respect to x^{μ} . Equation (5) has a simple physical interpretation: it describes single-particle driven diffusion on an N -dimensional curved space $\{x^{\mu} \mid \mu = 1, 2, \dots, N\}$. The form of the driving term in (6) comes from the Hamiltonian (1) and the kinetic constraint. But the curvature of this space is due solely to the kinetic constraint: from the form of a Fokker-Planck equation on a curved manifold [22] we identify the inverse metric tensor of this space as $g^{\mu\nu}(x) = \delta^{\mu\nu} \mathcal{C}_{\mu}(x)$. Thus the metric reads

$$g_{\mu\nu}(x) = \delta_{\mu\nu} \mathcal{C}_{\mu}^{-1}(x). \quad (7)$$

No summation is implied. The effect of dynamic facilitation is to endow the configuration space x with a nontrivial metric. Since dynamic facilitation is responsible for the interesting dynamical properties of these models, we expect that these dynamical properties can be extracted from the metric tensor.

The effect of the metric on configuration space trajectories is made clearer by writing a formal solution to equation (5) [23]:

$$P(x_b, t_b | x_a, t_a) = \int_a^b \sqrt{|g|} \mathcal{D}x e^{-\mathcal{S}[x]}, \quad (8)$$

where $P(x_b, t_b | x_a, t_a)$ is the conditional probability that a system starting at point x_a in configuration space at time t_a is found at point x_b at time t_b . We have introduced the determinant of the metric, $|g| \equiv \det(g_{\mu\nu}) = \prod_{\mu} \mathcal{C}_{\mu}^{-1}$. The path integral (8) is taken over all configurations of the system, weighted by the dynamic action $\mathcal{S}[x]$. Up to constant terms this action reads

$$\mathcal{S}[x] = \frac{1}{T} (H[x_b] - H[x_a]) + \frac{1}{T} \int_{t_a}^{t_b} dt \left(\dot{x}^{\mu} g_{\mu\nu} \dot{x}^{\nu} + \frac{\partial H}{\partial x^{\mu}} g^{\mu\nu} \frac{\partial H}{\partial x^{\nu}} \right), \quad (9)$$

where dots denote differentiation with respect to time, and the summation convention for once-repeated upper and lower indices is implied.

The action (9) weights the configuration space trajectories of our system. The system's classical trajectory, i.e. the path taken by the dynamics when $T \rightarrow 0$, is one of extremum \mathcal{S} . At finite T , stochastic fluctuations cause perturbations about this path. Equation (9) shows clearly the way the various ingredients of a dynamically facilitated model influence its trajectory through configuration space. The first term depends only on the Hamiltonian (1) evaluated at the endpoints. It gives rise to Boltzmann weights in the path integral (8) and plays no role in choosing the trajectory of the system. The path is chosen by a competition between the two terms in the integral of Eq. (9). The first term, $\mathcal{S}_1 \equiv T^{-1} \int dt \dot{x}^{\mu} g_{\mu\nu} \dot{x}^{\nu}$, is purely geometrical. It is the action for free motion in a curved background. It depends on the metric $g_{\mu\nu}$, and therefore on \mathcal{C}^{-1} . The second term, $\mathcal{S}_2 \equiv T^{-1} \int dt \partial_{\mu} H g^{\mu\nu} \partial_{\nu} H$, depends on the Hamiltonian (1), but is proportional to the inverse metric $g^{\mu\nu}$, and so to \mathcal{C} . At low temperatures, we expect \mathcal{S}_2 to be important only far from equilibrium, when mobility is plentiful—or equivalently, when the magnitudes of the coordinates $|x^{\mu}|$ are large and \mathcal{C} is large—and the system's relaxation will take place by way of gradient descent on the energy surface. When mobility has diminished significantly the constraints \mathcal{C} become small. We then expect

\mathcal{S}_1 to dominate. Hence the classical trajectory of the system in the region of weak dynamic facilitation will be governed by extremum \mathcal{S}_1 . This corresponds to the equation of a geodesic [24]:

$$\ddot{x}^\mu + \Gamma_{\alpha\beta}^\mu \dot{x}^\alpha \dot{x}^\beta = 0. \quad (10)$$

The Christoffel symbols $\Gamma_{\alpha\beta}^\mu$ are defined as $\Gamma_{\alpha\beta}^\mu \equiv \frac{1}{2}g^{\mu\nu}(g_{\nu\alpha,\beta} + g_{\beta\nu,\alpha} - g_{\alpha\beta,\nu})$, and the metric tensor raises and lowers indices. Equation (10) tells us how the kinetic constraint controls the system's trajectory in configuration space in the dynamically constrained regime. When mobility is scarce, the constraint \mathcal{C} is small, and the metric distance between points in configuration space, $s_{ab} \equiv \int_a^b \sqrt{g_{\mu\nu} dx^\mu dx^\nu}$, is large, by virtue of (7). By minimising this distance, and so following Eq. (10), we expect the system to follow a path that does not lead directly to a configuration of lowest energy. This is a geometrical interpretation of dynamical arrest.

3 A simple example

We now illustrate these ideas with a simple example. We define a model of two variables, $\{x^\mu\} = \{x, y\}$, with each variable constraining the other. Although such a model cannot exhibit true glassiness it is useful because we can visualise directly the two-dimensional configuration space it inhabits. We choose the Hamiltonian (1) to be quadratic,

$$H = \frac{J}{2} (x^2 + y^2), \quad (11)$$

where J sets the energy scale. We choose the constraint functions to be quadratic also, with each coordinate constraining the other:

$$\mathcal{C}_x = y^2, \quad \mathcal{C}_y = x^2. \quad (12)$$

Thus, the Fokker-Planck equation (5) is determined. Equation (7) gives the metric of this system as

$$g_{\mu\nu} = \begin{pmatrix} 1/y^2 & 0 \\ 0 & 1/x^2 \end{pmatrix}. \quad (13)$$

The metric is singular, and so distances in this configuration space become very large, when x or y vanish, reflecting the tendency of the kinetic constraint to suppress the dynamics of the system in the regime of low mobility. The space described by this metric is negatively curved with curvature scalar $R = -4(x^2/y^2 + y^2/x^2)$ [24]. The geodesics follow from (10) which in this case read

$$y\ddot{x} + (y/x)^3 \dot{y}^2 - 2\dot{x}\dot{y} = 0, \quad x\ddot{y} - (x/y)^3 \dot{x}^2 - 2\dot{x}\dot{y} = 0. \quad (14)$$

To illustrate the effect of the kinetic constraint on the trajectories chosen by the system we first cast Equation (5) into a form more convenient for numerical simulation. In the usual way [25] we recognize that (5) is equivalent to the coupled Langevin equations

$$\begin{pmatrix} \dot{x}(t) \\ \dot{y}(t) \end{pmatrix} = - \begin{pmatrix} Jy^2(t)x(t) \\ Jx^2(t)y(t) \end{pmatrix} + \begin{pmatrix} |y(t)|\eta_1(t) \\ |x(t)|\eta_2(t) \end{pmatrix}, \quad (15)$$

where the Gaussian white noise variables $\eta_i(t)$ have zero mean and variance $\langle \eta_i(t)\eta_j(t') \rangle = 2T\delta(t-t')\delta_{ij}$. In this representation the kinetic constraint manifests itself as a state dependent rate: the driving term is linear in \mathcal{C} while the noise term goes as $\sqrt{\mathcal{C}}$. The unconstrained version of the same model, i.e. one for which $(\mathcal{C}_x, \mathcal{C}_y) = (1, 1)$, would have Langevin equation $\dot{x}^\mu(t) = -Jx^\mu + \eta^\mu(t)$.

We now show explicitly that low temperature trajectories with fixed initial and final configurations are approximated by the geodesic equation (14). We have used Transition Path Sampling (TPS) [26] to ensure that we obtained a set of trajectories which both obeyed the endpoint conditions and were well-sampled from the dynamical action (9). In order to generate out-of-equilibrium trajectories for the relaxation from high energy configurations we used the Crooks-Chandler [27] algorithm; alternatives such as the local algorithm of Ref. [28] are also suitable.

Figure 1 presents the comparison of the dynamical evolution of our toy KCM with the geometry of its configuration space. TPS was used on the system defined by Eq. (15) to generate trajectories between the configurations indicated by a star. In Fig. 1a we show both a characteristic trajectory (thin red path) and the average over the set of all trajectories obtained via TPS (thick blue path). We also show geodesics (black curves) joining the final configuration to the initial configuration (indicated by a star), and to other configurations along the gradient descent path (indicated by black squares). The solutions to (14) are degenerate: there is one geodesic going left from the initial point and another going right. The distinction depends on the initial conditions on the path. In the TPS simulations we force the initial displacement to be to the left to obtain a set of trajectories which follows the left hand geodesics. These are the paths shown in Fig. 1a and 1b. In Fig. 1b we also show the average over a small set of right hand TPS trajectories and the corresponding pairs of geodesics.

In Fig. 1 we see the features described in the previous section. Initially the system is in the high energy region and it relaxes approximately by gradient descent. As it reaches the region of weak dynamic facilitation at low energies, the system relaxes by following approximately the geodesics of configuration space. Shown for comparison in Fig. 1a are the trajectories followed by an unconstrained version of the same model (dashed green path). In this case relaxation is by gradient descent. Given that the rate for motion in the x (resp. y) direction vanishes when y (resp. x) vanishes, trajectories have to cross the coordinate axis orthogonally, which gives trajectories (and geodesics) a “rectangular” shape. Equipotential lines are concentric circles, and the conflict between allowed dynamical paths and energy relaxation is evident.

4 An even simpler example

We can gain more insight into the nature of dynamic facilitation by considering an even simpler, one-variable model. This can be thought of as modeling facilitated dynamics for an order parameter, rather than for microscopic variables. Equations (5) and (6) tell us that an N -variable, dynamically constrained system looks like a single particle diffusing in N space dimensions. Thus a one-variable dynamically constrained model looks like a single particle diffusing in one space dimension. We can exploit the fact that one dimensional spaces are always flat [24] to ‘remove’ the kinetic constraint. We will see below that this can be done at the expense of introducing an effective free energy barrier.

Consider a model with one degree of freedom, x , with Hamiltonian (1) $H = Jx^2/2$. We choose the dynamical constraint to be $\mathcal{C}(x)$. This differs from the higher-dimensional cases in that the variable constrains itself. Consequently, the transformation from Fokker-Planck to Langevin form is ambiguous [25], and depends on whether one chooses pre-point or mid-point discretisation of time-dependent quantities (Itô or Stratonovich calculus). We choose the former, so that our model is causal. The Langevin description of our one-variable model is then

$$\dot{x}(t) = -Jx\mathcal{C}(x) + T\mathcal{C}'(x) + \sqrt{\mathcal{C}(x)}\eta(t), \quad (16)$$

where the prime denotes differentiation with respect to x , and the noise term $\eta(t)$ has zero mean and variance $\langle \eta(t)\eta(t') \rangle = 2T\delta(t-t')$. Since in this case the constraint depends on the variable it constrains, the second term on the right hand side of (16) is needed to ensure an equilibrium density proportional to $\exp(-Jx^2/2T)$ [29]. In the higher-dimensional cases we considered above there was no self-facilitation and

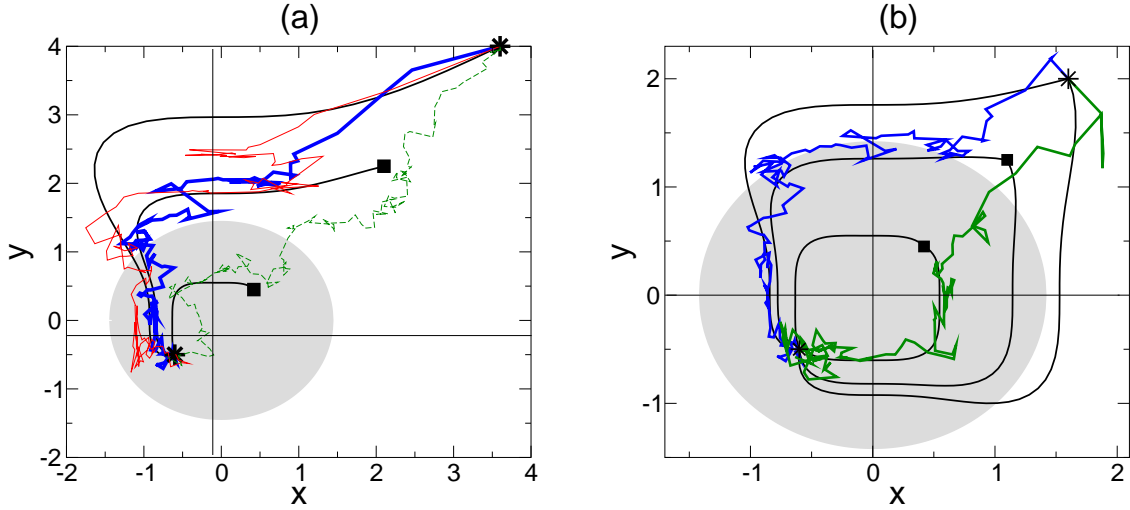


Figure 1: Configuration space trajectories for the toy model described in the text. Panel (a): $T = 2.0$, $J = 1$, $t_b - t_a = 129$, $(x_a, y_a) = (3.6, 4.0)$, $(x_b, y_b) = (-0.6 \pm 0.01, -0.5 \pm 0.01)$. We used TPS with the Crooks-Chandler [27] algorithm to generate 2.78×10^8 trajectories, starting from point a (indicated by a star at the top right), of which 11403 landed in the end-point b (indicated by a star at the bottom left). The thin red path is a representative trajectory. The thick blue path is the mean of those trajectories. The dashed green path is the mean of 273 trajectories reaching b from a for an unconstrained version of an otherwise identical model. Numerical solutions to the geodesic equation (14) joining b to three other points (shown as black squares) are overlaid. The gray circle encloses the equilibrium region $\langle x^2 + y^2 \rangle = T/J$. Panel (b): a similar plot starting from $(x_a, y_a) = (1.6, 2.0)$. Again, 2.78×10^8 trajectories were generated. The thick blue path shows the mean of 2199 trajectories landing in region b which follow the left hand side route. The average path over 6 right hand side trajectories is also shown in green.

this term was absent. The corresponding unconstrained model has $\mathcal{C}(x) = 1$, and its Langevin equation is $\dot{x}(t) = -\partial_x(Jx^2/2) + \eta(t)$.

The appearance of the multiplicative noise term $\sqrt{\mathcal{C}(x)}\eta(t)$ in Eq. (16) is due to the metric-augmented diffusion term in (6), and is therefore a consequence of the kinetic constraint. The statement that a one-dimensional space is flat is equivalent to the statement that the noise may be made additive by a local change of variables. If we make the change of variables

$$y(t) \equiv \int^{x(t)} \frac{dx'}{\sqrt{\mathcal{C}(x')}}, \quad (17)$$

we can use Itô's formula [25] to rewrite (16) as

$$\dot{y}(t) = -Jx\sqrt{\mathcal{C}(x)} + \frac{1}{2}T\sqrt{\mathcal{C}(x)}\partial_x \ln \mathcal{C}(x) + \tilde{\eta}(t), \quad (18)$$

where x should be eliminated in favour of y . The noise $\tilde{\eta}(t)$ has the same mean and variance as $\eta(t)$. Provided we can write the deterministic terms in (18) as the gradient of an effective potential we can regard Equation (18) as unconstrained, in the sense that the prefactor of the noise does not contain the dependent variable.

Consider the specific case of a quadratic constraint, $\mathcal{C}(x) = x^2$. Equation (16) becomes

$$\dot{x} = -Jx^3 + 2Tx + x\eta, \quad (19)$$

where we have assumed $x > 0$. The change of variables (17) now amounts to a Cole-Hopf transformation, $y \equiv \ln x$. Hence the regime where dynamic facilitation is relevant corresponds to $y \ll 0$. Equation (18) now reads

$$\dot{y} = -\partial_y \left(\frac{J}{2} e^{2y} - Ty \right) + \tilde{\eta}. \quad (20)$$

Equation (20) looks like an unconstrained model with an effective *entropic* barrier $\Delta F = -Ty = -T \ln x$, which prevents the particle from accessing the dynamically constrained regime of $y \ll 0 \Rightarrow x \sim 0$ [30]. Figure 2 illustrates this.

5 Conclusions

In this paper we have presented a geometric interpretation of dynamic facilitation. By generalizing kinetically constrained models to continuous degrees of freedom we have shown that in these systems the kinetic constraints can be seen as endowing configuration space with a non-trivial metric structure. This metric structure in turn determines the dynamical trajectories. In the regime where the kinetic constraint is dominant, i.e. at low temperatures or energies, the geometry forces the dynamics to proceed through paths close to geodesics, rather than close to paths which relax the energy. This conflict between available paths and energy relaxation gives rise to dynamical bottlenecks or barriers, despite the fact that there are no static barriers in these systems.

Our view of dynamical arrest in terms of the geometry of configuration space is distinct from that based on the idea of motion in an effective rugged energy (or free energy) landscape (see [3] and references therein). In the landscape perspective it is often assumed that relevant features of the energy surface, like local minima and saddle points, determine the behaviour of the system, and that knowledge of the statistical properties of these features is sufficient to explain both dynamic and thermodynamic properties. In our approach the effective energy surface displays no particular features, the thermodynamics is uninteresting, and there are

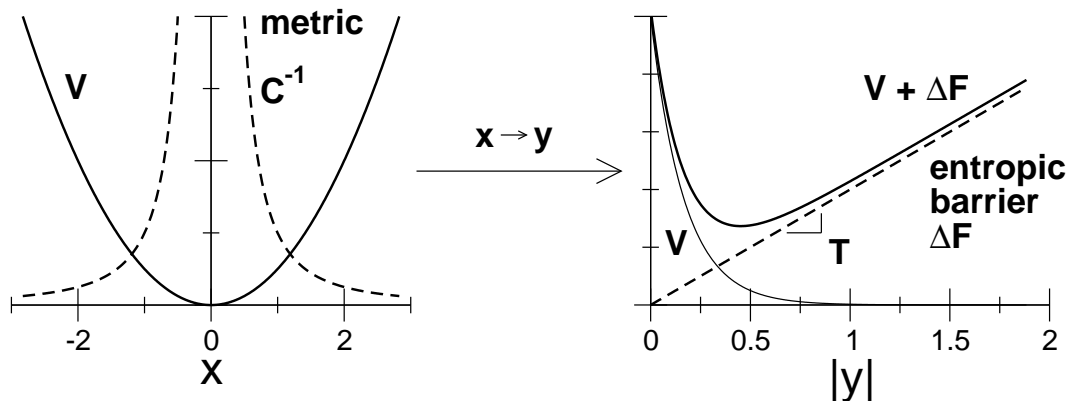


Figure 2: An illustration of how a constrained problem may have an alternative representation as an unconstrained one with an extra free energy barrier (from the example of section 4). The constraint $\mathcal{C}(x)$ fixes the metric $g(x) = \mathcal{C}^{-1}(x)$ of space x . This implies that metric distances become large in the region of small x . Under the transformation Eq. (17) the problem changes into a non constrained one, $g(y) = 1$, but with an extra free energy barrier $\Delta F(y)$ which excludes the system from the low energy region of large $|y|$.

no special configurations, such as local minima or saddles, which play any major roles either in the statics or in the dynamics. All the interesting structure is in the paths between configurations, and therefore in the dynamics. In this picture it is the effective metric structure of configuration space that distinguishes a glassy system from a normal one, and not the ruggedness of its energy surface.

We are grateful to D. Chandler for discussions. We acknowledge financial support from EPSRC Grants No. GR/R83712/01 and GR/S54074/01, the Glasstone Fund, and Linacre College Oxford.

References

- [1] C.A. Angell, Science **267**, 1924 (1995).
- [2] M.D. Ediger, C.A. Angell and S.R. Nagel, J. Phys. Chem. **100**, 13200 (1996).
- [3] P.G. Debenedetti and F.H. Stillinger, Nature **410**, 259 (2001).
- [4] J.P. Garrahan and D. Chandler, Phys. Rev. Lett. **89**, 035704 (2002); Proc. Natl. Acad. Sci. USA **100**, 9710 (2003).
- [5] L. Berthier and J.P. Garrahan, J. Chem. Phys. **119**, 4367 (2003); Phys. Rev. E **68**, 041201 (2003).
- [6] S. Whitlam, L. Berthier, and J.P. Garrahan, e-print cond-mat/0310207 (2003).
- [7] L. Berthier, e-print cond-mat/0310210 (2003).
- [8] Y. Jung, J.P. Garrahan and D. Chandler, e-print cond-mat/0311396 (2003).
- [9] H. Sillescu, J. Non-Cryst. Solids **243**, 81 (1999).

- [10] M.D. Ediger, *Annu. Rev. Phys. Chem.* **51**, 99 (2000).
- [11] S.C. Glotzer, *J. Non-Cryst. Solids*, **274**, 342 (2000).
- [12] K. Schmidt-Rohr and H. Speiss, *Phys. Rev. Lett.* **66**, 3020 (1991); M.T. Cicerone and M.D. Ediger, *J. Chem. Phys.* **103**, 5684 (1995); E.V. Russell et al., *Phys. Rev. Lett.* **81**, 1461 (1998); L.A. Deschenes and D.A. Vanden Bout, *Science* **292**, 255 (2001).
- [13] T. Muranaka and Y. Hitawari, *Phys. Rev. E* **51**, R2735 (1995); D. Perera and P. Harrowell, *Phys. Rev. E* **51**, 314 (1995); B. Doliwa and A. Heuer, *Phys. Rev. Lett.* **80**, 4915 (1998); C. Donati et al., *Phys. Rev. E* **60**, 3107 (1999).
- [14] E. Weeks et al., *Science* **287**, 627 (2000).
- [15] S.H. Glarum, *J. Chem. Phys.* **33**, 639 (1960).
- [16] R.G. Palmer, D.L. Stein, E. Abrahams and P.W. Anderson, *Phys. Rev. Lett.* **53**, 958 (1984).
- [17] G.H. Fredrickson and H.C. Andersen, *Phys. Rev. Lett.* **53**, 1244 (1984).
- [18] F. Ritort and P. Sollich, *Adv. in Phys.* **52**, 219 (2003).
- [19] J. Jäckle and S. Eisinger, *Z. Phys.* **B84**, 115 (1991).
- [20] W. Kob and H.C. Andersen, *Phys. Rev. E* **48**, 4364 (1993).
- [21] For other perspectives on glassiness also based on curved spaces, but with a different microscopic origin, see for example: P.J. Steinhardt, D.R. Nelson and M. Ronchetti, *Phys. Rev. Lett.* **47**, 1297 (1981) and D.R. Nelson, *Phys. Rev. B* **28**, 5515 (1983).
- [22] H. Risken, “The Fokker-Planck equation: Methods of solution and Applications”, (Springer Verlag, New York, 1984).
- [23] J. Zinn-Justin, “Quantum Field Theory and Critical Phenomena”, (OUP, Oxford 1989).
- [24] C.W. Misner, K.S. Thorne, and J.A. Wheeler, *Gravitation*, W.H. Freeman and Company, San Francisco (1973).
- [25] N.G. Van Kampen, “Stochastic Processes in Physics and Chemistry”, (North-Holland, Amsterdam, 2001).
- [26] P.G. Bolhuis, D. Chandler, C. Dellago and P.L. Geissler, *Ann. Rev. Phys. Chem.* **59**, 291 (2002).
- [27] G.E. Crooks and D. Chandler, *Phys. Rev. E* **64**, 026109 (2001).
- [28] L.R. Pratt, *J. Chem. Phys.* **85**, 5045 (1986).
- [29] In the Itô convention, the Fokker-Planck equation for the Langevin equation (16) is $\partial_t P(x, t) = \partial_x [J x \mathcal{C}(x) P(x, t) - T \mathcal{C}'(x) P(x, t)] + T \partial_x^2 [\mathcal{C}(x) P(x, t)]$. The right hand side of this equation can be rewritten as $\partial_x \{ \mathcal{C}(x) [J x P(x, t) + T \partial_x P(x, t)] \}$, leading to the equilibrium density $P_{\text{eq.}}(x) \propto \exp(-Jx^2/2T)$, which is indeed independent of the constraining function $\mathcal{C}(x)$. If the Stratonovich convention is used, the second term in the right hand side of Eq. (16) is then preceded by a factor 1/2, giving the same Fokker-Planck equation as above.

[30] The equilibrium density in the y representation is $P_{\text{eq.}}(y) \propto \exp(-Je^{2y}/2T + y)$. This corresponds to the density $P_{\text{eq.}}(x)$ after the change of variables $x \rightarrow y = \ln x$, as can be seen from the invariance of the partition function: $Z = \int \exp(-Jx^2/2T) dx = \int \exp(-Je^{2y}/2T) e^y dy$.